

**SINGS: The Spitzer Infrared Nearby Galaxies Survey**  
**First Data Delivery**  
**October 2004**

**USER'S GUIDE**

**1. Introduction**

This document describes the first data delivery of the Spitzer Legacy program SINGS. It is organized as follows: section 2 lists the data products contained in this delivery and their general characteristics; sections 3, 4, and 5 provide a description of the post-BCD processing for IRAC, MIPS, and IRS data, respectively; finally, section 6 briefly describes the data reduction steps of the ancillary data associated with this delivery.

For a complete description of the SINGS program, galaxy sample, and observing strategy, please refer to Kennicutt et al. 2003, PASP, 115, 928.

**2. Content of the Data Delivery**

**2.1 First-Delivery Sample and Data Products**

The SINGS sample contains 75 galaxies, representative of a large range of properties of local normal galaxies (Kennicutt et al. 2003). Of these 75, 8 are in the present delivery (10% of the sample). The eight galaxies, all observed with both IRAC and IRS, were chosen to be a cross-cut of the SINGS sample, i.e., to cover as much as possible a large range of morphological types and IR/optical ratio, within the constraints of the galaxy sample that was observed at the time the data were prepared. The table below lists the galaxies and summarizes the data products delivered for each:

Name	Morph.	Reason for Selection	Spitzer Data Products			Ancillary Data Products	
			IRAC	MIPS	IRS	Optical Images	Optical Spectra
NGC0337	SBd	Morphology	4 mosaics	x	1D, Low+High	BVRIH $\alpha$	1D, nuc. & 20'' scan
NGC2798	SBa	High IR/Opt	4 mosaics	x	1D, Low+High	BVRIH $\alpha$	1D, nuc. & 20'' scan
NGC3198	SBc	Morphology	4 mosaics	x	1D, Low+High	BVRIH $\alpha$	1D, nuc. & 20'' scan
NGC4725	SABab	Low IR/Opt	4 mosaics	x	1D, Low+High	BVRIH $\alpha$	1D, nuc. & 20'' scan
NGC4826	SAab	Morphology	4 mosaics	x	1D, Low+High	BVRIH $\alpha$	1D, nuc. & 20'' scan
NGC5194	SABbc	Community Interest	4 mosaics	x	1D, Low+High	BVRIH $\alpha$	1D, nuc. & 20'' scan
NGC5408	IBm	Morphology	4 mosaics	x	1D, Low+High	Not avail	Not avail
NGC7331	SAb	Validation target	4 mosaics	3 mosaics	1D, Low+High	BVRIH $\alpha$	1D, nuc. & 20'' scan

### 2.1.1 IRAC Mosaics

IRAC data products are delivered for all 8 galaxies. For each galaxy, 4 mosaics, one for each of the four IRAC bands, are delivered as single-extension FITS files. The pixel scale of the mosaics is approximately 0.75 arcsec, and the flux scale is MJy sr<sup>-1</sup>.

Details of the post-BCD processing are given in Section 3.

### 2.1.2 MIPS Mosaics

The main campaign of MIPS observations for SINGS only began recently, and hence MIPS mosaics in all three bands are only delivered for NGC7331. This galaxy is the SINGS validation target. As in the previous case, each mosaic is a single-extension FITS file. The pixel scale of the MIPS mosaics is wavelength-dependent: 0.75 arcsec at 24  $\mu$ m, 3.00 arcsec at 70  $\mu$ m, and 6.00 arcsec at 160  $\mu$ m. The flux scale is MJy sr<sup>-1</sup>.

Details on the post-BCD processing are given in section 4.

### 2.1.3 IRS One-dimensional Spectra

Both Low-resolution and High-resolution, one-dimensional (1D) spectra of the central 20''x15'' (High-res) to 50''x30'' (Low-res) are delivered for each of the 8 galaxies, in the wavelength range 5-15  $\mu$ m (Short-Low, SL, R=50-100), 15-37  $\mu$ m (Long-Low, LL, R=50-100), 10-20  $\mu$ m (Short-High, SH, R=600), 20-37  $\mu$ m (Long-High, LH, R=600). The fluxes are calibrated in MJy sr<sup>-1</sup> (Low-res) or Wm<sup>-2</sup> $\mu$ m<sup>-1</sup>sr<sup>-1</sup> (High-res). The data are provided as multiple ASCII files (.txt).

Details on the data format and content, and on the post-BCD processing for the spectra are given in section 5.

### 2.1.4 Optical Images/Mosaics

Optical imaging data in the standard B, V, R, I broad-band filters and in narrow-band filters at the wavelength of the H $\alpha$ + [NII] emission are delivered for 7 of the 8 galaxies (there are no optical imaging data for NGC5408).

The images are either single pointings, or mosaics of 2 or more adjacent and partially-overlapping frames. **None** of the images is background-subtracted, and the narrow-band images are **not** continuum-subtracted.

All optical data are single extension FITS file (one file for each filter); they are flux calibrated and have astrometric solutions. Photometric and astrometric keywords are stored in the FITS headers.

The pixel scale is 0.305 arcsec (KPNO data) or 0.433 arcsec (CTIO data). The images all have NE orientation. The flux scale is count/sec (CPS), and the relevant photometric keywords are: PHOTFLAM, to convert CPS to Jy, and ZPOINT, for the zeropoint.

More details on the optical images are given in section 6.1.

### *2.1.5 Optical One-dimensional Spectra*

One-dimensional (1D) spectra in the wavelength range 0.36-0.70  $\mu\text{m}$  are delivered for 7 of the 8 galaxies (there are no spectroscopic data available for NGC5408). For each galaxy, two spectra are delivered: the nuclear spectrum and the central 20''x20'' drift-scan spectrum.

The nuclear spectra are 2.5''x2.5'' (KPNO) or 2.5''x3.0'' (CTIO) aperture extractions of the brightest few central pixels. The 20''x20'' drift-scan spectra target the central region of each galaxy, in a similar fashion to some of the IRS spectra. Both type of optical spectra are wavelength and flux calibrated. Resolution is  $\sim 8$  Angstrom, and all fluxes are corrected for foreground Galactic extinction.

Nuclear and drift scan spectra are stored in separate ASCII files (\*.txt). More details on the data are given in section 6.2.

## **2.2 File Name Convention**

For each galaxy, multiple datasets are delivered, with the following filename convention:

- *IRAC mosaics*: ngcXXXX\_v03\_1\_irac#.fits (with #=1,2,3,4; e.g., ngc0337\_v03\_1\_irac1.fits)
- *MIPS mosaics*: ngcXXXX\_mips#.fits (with #=24,70,160; e.g., ngc7331\_mips24.fits)
- *IRS Low-Res 1D spectra*: ngcXXXX\_md#\_tp.txt (md=SL,LL; #=1,2; tp=sp,bg)
- *IRS High-Res 1D spectra*: ngcXXXX\_md\_sp.txt (md=SH,LH)
- *Optical images/mosaics*: ngcXXXX\_#.fits (with #=B,V,R,I,Ha, e.g., ngc5194\_Ha.fits)
- *Optical 1D spectra*: ngcXXXX\_nuclear\_002\_5.txt and ngcXXXX\_drift\_020\_020.txt.

## **IRAC Data Products and Post-BCD Processing**

### **3.1 Introduction**

The SINGS IRAC images are created from multiple Spitzer images in either a mosaic or single field dither pattern. The fundamental data used for these are the Basic Calibrated Data (BCD) images produced by the Spitzer Science Center (SSC). These data have already undergone a number of processing steps including conversion from engineering to scientific units, flat fielding and bias subtraction. The SINGS IRAC pipeline further processes these data to deal with a number of issues including frame geometric distortion and rotation, residual flat fielding, cosmic rays, frame alignment and bias drift. Frames are finally combined using the drizzle algorithm to maximize resolution from the individual sub-sampled images. The major observation and processing steps are detailed below.

### **3.2 Data Products**

The IRAC data products contained in this delivery are single-extension FITS files, one file for each IRAC band (\*.irac1.fits, \*.irac2.fits, etc.). The images are calibrated in MJy sr<sup>-1</sup>, and have pixel size of approximately 0.75 arcsec.

The original header keywords are retained, plus others added as a result of the post-BCD processing. In particular, astrometry is stored using FITS standard WCS coordinate keywords; the flux scale is stored in the BUNIT keyword; and the background subtraction and its value are stored in the keywords BACK\_SUB (performed=T, not performed=F) and BACKGRND (value), respectively. In this first delivery, all BACK\_SUB=F and BACKGRND=0. for the IRAC mosaics.

### **3.3 Observational Strategy**

Observations were carried out in accordance with the SINGS IRAC observing strategy (Kennicutt et al. 2003). For galaxies larger than the 5' size of the IRAC detectors, observations are taken in a mosaic pattern, offsetting the field of view by ~50% each time. This process is repeated twice, with observations separated by at least 24 hours to best correct for asteroids and detector artifacts. Points in the central mosaic regions are thus imaged eight times and the outermost regions four times. Galaxies fitting in a single IRAC field are imaged using two sets of four dithered observations, again resulting in points being observed eight times over the bulk of the final images. Observations are 30 seconds in duration with an additional one second exposure taken at each pointing to provide data in cases where the main observation is saturated.

### **3.4 Image Processing**

The steps performed by the SINGS IRAC pipeline are the following:

#### *a. Geometric Distortion and Image Rotation*

BCD images contain geometric distortions caused by IRAC's off-axis location in the Spitzer focal plane. The magnitude of these distortions is up to 2.2". These are corrected for in the SINGS IRAC pipeline using coefficient tables obtained from the GOODS team. Frames (single-exposure images) from the second set of exposures are also rotated to the

orientation of the first using the header position angle difference between the first images of each observation set.

#### *b. Bias Structure*

At present there is some residual bias structure in the IRAC BCD data, particularly affecting band 3. To address this issue, IRAC band 3 frames for galaxies observed with a mosaic pattern are median combined and the result subtracted from each frame. This method is not applied to observations obtained with a dither pattern (small galaxies), as in this case the object occupies a large fraction of each frame, thus strongly affecting the median.

#### *c. Image Offsets*

Offsets between individual BCD images are determined through image cross-correlation. In this process, rough cosmic ray rejection is first carried out by comparing the short and long IRAC exposures at each pointing. Geometric distortion corrections are also applied. Any two frames with at least 10,000 pixels in common are cross-correlated with each other. Individual frame pair cross-correlation results from all four bands are combined for maximal accuracy, weighting offsets by their errors and applying outlier rejection. Within each band, a consistent solution for frame positions is then obtained through least square fitting. Accuracy for this process varies from galaxy to galaxy, but is generally in the range 0.1-0.2 pixels.

#### *d. Bias Drift*

IRAC images are at present still subject to full frame DC bias drift with time. To correct for this, the SINGS IRAC pipeline matches the median flux level in regions of overlap and determines any DC offset between overlapping frames. This offset is assumed to be due to the bias drift.  $\chi^2$  minimization is again applied to find a consistent solution for all frames and the appropriate DC offsets applied. It should therefore be noted that a small unphysical offset may be present in the SINGS IRAC images.

#### *e. Cosmic Rays*

Final cosmic ray masks are created using standard drizzle methods (see the HST Dither Handbook: [http://www.stsci.edu/instruments/wfpc2/Wfpc2\\_driz/dither\\_handbook.html](http://www.stsci.edu/instruments/wfpc2/Wfpc2_driz/dither_handbook.html)). Each image is first drizzled to correct for geometric distortion. The weight files from this step are also used to create pixel masks. Following this, the images are median combined to reject cosmic rays. These images are then 'blotted' - a step that effectively reverses the steps so far - to create images equivalent to the original input images but without cosmic rays. Finally, a spatial derivative is calculated to assess the effects of blurring in the median image (Dither Handbook, page 60) and the original and blotted images are compared to obtain a cosmic ray mask for each image.

#### *f. Final Images*

The final step in the SINGS IRAC pipeline is to drizzle the original long exposures together, applying the geometric distortion and rotation corrections, cosmic ray masks and determined image offsets. In this process, the output pixels are scaled to be 0.625

times that of the input pixels, yielding a size of approximately 0.75 arcsec per pixel. A drop-size of 0.75 input pixels is applied. These values are chosen to yield fully sampled images with maximal resolution. A correction factor is also applied to the final images to maintain accurate photometry given the change in pixel size.

This latter step combines together the images from the two different AORs, thus removing asteroids in the process.

### **3.5 Known Errors and Image Artifacts**

In using the final images, users should be aware that at present the astrometry between bands has not been made fully consistent. As such, there may exist small offsets in object world coordinates between bands, typically less than 1 pixel ( $\sim 0.75''$ ), with occasional peak of 2 pixels.

Also, as mentioned earlier, small background level corrections have been applied to individual frames to correct for bias drift, potentially leading to an unphysical offset in the final images (i.e., slightly negative backgrounds).

Finally, users are cautioned to be aware of standard IRAC detector artifacts that may also be present in the SINGS data. These are detailed extensively elsewhere (Hora et al. 2004, SPIE, in press; Fazio et al. 2004, ApJS 154, 10) and include: persistent images in channels 1 and 4, diffuse stray light, stray light from point sources, Muxbleed, column pulldown and banding, remaining full-frame bias, ghost images, and extended-source calibration errors. Because we combine two epochs of observations that are slightly rotated and we match the backgrounds between overlapping BCD images, some of the detector anomalies are mitigated in our final mosaics.

## **4. MIPS Data Products and Post-BCD Processing**

### **4.1 Introduction**

The SINGS MIPS mosaics in this delivery were created from multiple Spitzer images obtained in scan-mapping mode, and fully processed with the MIPS Data Analysis Tool (MIPS DAT, Gordon et al. 2004, PASP, submitted, <http://mips.as.arizona.edu/mipspage/dat.pdf>). The major observation and processing steps are detailed below.

### **4.2 Data Products**

The MIPS data products contained in this delivery are single-extension FITS files, one file for each MIPS band (\*\_mips24.fits, \*\_mips70.fits, and \*\_mips160.fits). The images are calibrated in MJy sr<sup>-1</sup>, and have pixel size 0.75, 3.00 and 6.00 arcsec for the 24  $\mu$ m, 70  $\mu$ m, and 160  $\mu$ m mosaics, respectively. The pixel sizes of the MIPS mosaics have been chosen to adequately sample the point spread function and at the same time be a multiple of the IRAC mosaics pixel scale (approximately 0.75 arcsec, see section 3). Backgrounds have been subtracted out of the 24 and 70  $\mu$ m data as part of the data processing. The 160  $\mu$ m data, however, do not include background subtraction.

All original fits header information has been retained. The headers' content has been re-arranged so that basic information on the observations, the target, and coordinates, and the pixel values appears first in the listing. Among the relevant keywords: the mosaics' astrometry is stored in the standard FITS WCS keywords; the flux units are stored in ZUNITS; and, like for the IRAC images, the background subtraction and its value are stored in the keywords BACK\_SUB (performed=T, not performed=F) and BACKGRND (value), respectively. All other information, which includes details on the observations and the data processing, is located after these basic keywords.

### **4.3 Observational Strategy**

The MIPS observations were obtained using the scan-mapping mode in two separate visits to the galaxy. Separate visits allow asteroids to be recognized and provide observations at orientations up to a few degrees apart to ease removal of detector artifacts. As a result of redundancy inherent in the scan-mapping mode, each pixel in the core map area was effectively observed 40, 20, and 4 times at 24, 70, and 160 microns, respectively, resulting in integration times per pixel of 160 s, 80 s, and 16 s, respectively.

### **4.4 Post-BCD Image Processing**

The MIPS data were processed using the MIPS DAT version 2.80 along with additional customized processing software. The processing steps are as follows.

1. For the 70 and 160  $\mu$ m data, a linear fit is applied to the ramps (the counts accumulated in each pixel during the non-destructive readouts), and slopes are derived. This step also removes cosmic rays and readout jumps.

2. The initial processing of the 24  $\mu\text{m}$  data is different from the 70 and 160  $\mu\text{m}$  data, as the 24  $\mu\text{m}$  data are received as already containing the slopes fitted to the ramps. Thus, the 24  $\mu\text{m}$  images are processed through a droop correction (that removes an excess signal in each pixel that is proportional to the signal in the entire array), correction for non-linearity in the ramps, and dark current subtraction.

3. Telescope optical signatures and time-dependent responsivity variations in the detector elements are removed from the data, in the following way:

- a. For the 24  $\mu\text{m}$  images, scan-mirror-position dependent and independent flatfields are applied to the data in two steps. First, scan mirror position dependent flats are created for off-target data in the scan map; these flats are the first ones applied to the data. Next, scan mirror position independent flats are created for off-target data, and these are the second type of flatfields applied to the data. Latent images in the 24  $\mu\text{m}$  data are masked out after this step.
- b. The stim flash frames taken by the telescope are used for responsivity corrections of the 70 and 160  $\mu\text{m}$  arrays. Next, the dark current is subtracted off, and illumination corrections are applied to the data. For the 70  $\mu\text{m}$  data, a time-dependent illumination correction is applied. Following this, stim flash latent images are subtracted from the 70  $\mu\text{m}$  data, which also results in a background subtraction.

4. Final mosaics are made from the individual frames. Note that the 24  $\mu\text{m}$  data from each AOR are mosaiced separately whereas the 70 and 160  $\mu\text{m}$  data from both AORs are mosaiced together. After mosaicing, backgrounds are subtracted from the two 24  $\mu\text{m}$  images in two steps. First, planes ( $z = Ax + By + C$ ) are fit to the background counts inside square regions centered on the galaxy and with size three times the galactic optical diameter. Pixels within the optical disk of the galaxy are excluded from the fit. After the fitting planes are subtracted, any residual offset is measured in regions near the optical disk and subtracted. The two mosaics are then averaged together to make a final 24  $\mu\text{m}$  mosaic.

5. After the mosaics are created, the images are multiplied by a final calibration factor that converts the MIPS units into  $\text{MJy sr}^{-1}$ . The calibration factors are derived after all processing steps have been applied to the mosaics. The factors are the following (keyword JANSscale in the image headers):

24  $\mu\text{m}$ :  $0.0439 \text{ MJy sr}^{-1} \text{ MIPS\_units}^{-1}$

70  $\mu\text{m}$ :  $634 \text{ MJy sr}^{-1} \text{ MIPS\_units}^{-1}$

160  $\mu\text{m}$ :  $42.6 \text{ MJy sr}^{-1} \text{ MIPS\_units}^{-1}$



## 4.5 Known Problems and Uncertainties

### *Drifts in the 70 $\mu\text{m}$ data*

The 70  $\mu\text{m}$  data contains short-term drift effects (where the background signal changes in strength) that have not been removed from these data. Work is underway to correct for this effect and improved versions of the maps will be delivered in a future data release.

### *Photometric Uncertainties*

Currently the estimated calibration uncertainties for MIPS extended object photometry are ~10% for the 24  $\mu\text{m}$  data and ~20% for the 70 and 160  $\mu\text{m}$  data.

## 5. IRS Data Products and Post-BCD Processing

### 5.1 Observations and Data Products

The IRS data products provided in this release consist of a single representative spectrum in each of the four IRS modules -- Short-Low (SL, 5-15  $\mu\text{m}$ , R=50-100), Long-Low (LL, 15-37  $\mu\text{m}$ , R=50-100), Short-High (SH, 10-20  $\mu\text{m}$ , R=600), and Long-High (LH, 20-37  $\mu\text{m}$ , R=600) -- for all 8 target galaxies. All SINGS IRS observations are taken in Spectral Mapping Mode, in which the slit is moved in a raster pattern to build up a redundantly-sampled spectral map of the target region. For this release, we are providing extractions of a rectangular region ranging in size from 22.6"x14.8" (SH) to 50"x33" (SL), centered on the nucleus of each galaxy. An example illustrating these extraction regions overlayed on the 8  $\mu\text{m}$  image of M51 is shown in Fig. 1. Also provided are matching interpolated spectral fits to the background for the SL observations (see below), and pure model predictions of the background spectra for the high-resolution observations.

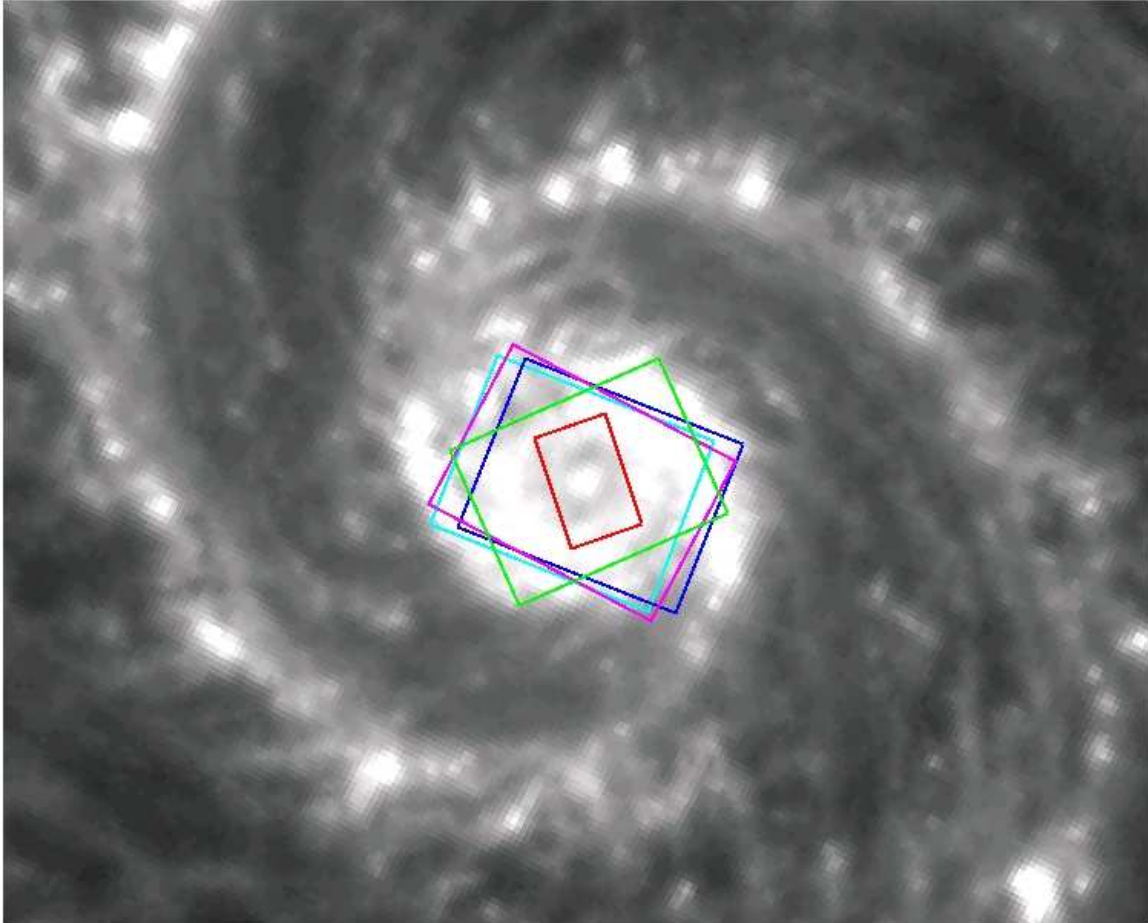


**Figure 1:** The 8  $\mu\text{m}$  image of M51, with the extraction regions for the IRS spectra in this delivery overlayed in color: magenta: SL, blue: LL1, cyan: LL2, green: LH, red: SH.

## 5.2 File Format and Naming Convention

All spectra are formatted as ASCII files in the IPAC table format. The brief headers give the date of each observation, corresponding to the first data collection event in the spectral map, as well as the location of the regions over which the data were extracted.

### *Low-Resolution*

Low resolution files are divided by module and order, with a naming convention `ngcXXXX_md#_tp.txt`, where "md" is the module, either "SL" or "LL", "#" is the order (1 or 2), and "tp" is the type, either "sp" for normal spectra or "bg" for background files. Each file consists of a header followed by the data in two columns: wavelength (in  $\mu\text{m}$ ), and flux intensity (in  $\text{MJy/sr}$ ).

### *High-Resolution*

High resolution files are divided by module, with a naming convention `ngcXXXX_md_sp.txt`, where "md" is the module, either "SH" or "LH". Each file consists of a header followed by the data in three columns: order (corresponding to the order of the spectrograph from which the data were obtained), wavelength (in  $\mu\text{m}$ ), and flux intensity ( $\text{W m}^{-2} \mu\text{m}^{-1} \text{sr}^{-1}$ ). The single background model for the SH+LH observations is available as `ngcXXXX_SHLH_bg.txt`.

## 5.3 Post-BCD Data Processing

### *Low-Resolution*

The low resolution spectral maps were assembled into three-dimensional spectral cubes using Cubism, a tool specifically designed for this purpose (see Kennicutt et al, 2003, Sect. 6.2, for more information). Bad pixels are flagged and removed in-situ in the redundantly sampled map (typically 10-30 per frame). A rectangular region of  $33'' \times 50''$  was used to extract the SL spectra. (An exception is for NGC7331, our validation galaxy, for which a smaller SL map was obtained, yielding a smaller extraction regions of  $50'' \times 16.5''$ ). The LL spectra were extracted from a similar area. Uncalibratable data at the ends of each order were trimmed from the final spectrum.

### *High-Resolution*

All 15 positions within the high-resolution maps were averaged together as 2D spectra, and the resulting average was extracted using the extraction core of Cubism. Time varying bad pixels, which respond to light, but vary on short timescales, dominate the noise in the high-resolution spectra, LH in particular. These pixels were manually flagged, typically numbering 100-200 in SH and 200-400 in LH, and rejected from the extraction. In all cases, noisy areas at the red and blue ends of each spectral order have been trimmed to create the final, averaged SH or LH spectrum. These are typically 5-25 pixels at the ends of the orders.

### *Background Subtraction*

The LL maps, assembled from long radial strips which extend  $10'$  or more across the galaxy, offer copious measurement of the nearby zodiacal and cirrus "background" (which actually is physically a foreground emission). Typically 10-14 spectral frames

were averaged together for subtraction in the 2D spectral image. This process not only removes the background, it also restores many unwieldy time-varying bad pixels to correct scales. The SL maps are much smaller, and do not typically extend beyond the extended emission of larger galaxies. However, since SL maps are executed one sub-slit at a time (SL1 and SL2 separately), for small galaxies, a deep map of the nearby background emission is obtained in the "outrigger" order. A suite of 15 background observations, taken from among the dedicated set and selected outrigger fields, was used to generate a 1D background spectrum. The template spectra were extracted to 1D, fit by low-order polynomials, and sorted according to the  $8\text{ }\mu\text{m}$  background flux predicted by the Reach et al. (2003, Icarus, 164, 384) models. The SL background for a given galaxy was computed by interpolating between the polynomial fits to the template spectra, using the Reach et al.'s  $8\text{ }\mu\text{m}$  background flux as the interpolant. Each SL spectrum was then background-subtracted using this noiseless interpolated fit.

For two galaxies, NGC5408 and NGC2798, the details of pipeline stray-light correction led to background-subtracted spectra which differed substantially from the spectra extracted using *in situ* backgrounds from the outrigger observations available for these small galaxies. In these two cases we have provided the direct 2D background-subtracted spectra, averaging together 18 outrigger spectra for subtraction, similar to the method employed for LL. The interpolated 1D background estimates, though unused, remain available.

The high-resolution maps have not had any background removed. Instead, model spectra from the Reach et al.'s model are given, applicable to the date of observation of each galaxy.

### *Flux Calibration*

The high-resolution average spectra were extracted directly against well-modeled standard calibration stars (e.g. HR 6688) using the unflatfielded "droop" product produced by the IRS pipeline. This direct "relative spectral response function" (RSRF) method minimizes dependencies on the pipeline flux calibration product. All low-res spectra were corrected for several factors which contribute to errors in the naively computed flux:

1. An Aperture Loss Correction Function (ALCF) which consists of a differential aperture correction to overcome the specific, narrowing aperture employed in the IRS pipeline.
2. A Slit Loss Correction Function (SLCF) which accounts for the fraction of light of the point source calibration standards which is admitted by the IRS slits, as a function of wavelength. Extended sources do not suffer the same fractional loss of light, and thus must be corrected down from the standard flux calibration, which assumes point sources.
3. An effective beam size of the slit which is used to convert per-pixel average flux in Jy to a flux intensity in MJy/sr. Since the beam profiles have not yet been measured, a square sided profile was assumed, with slight adjustment to match matched-aperture photometry obtained from IRAC (all 8 galaxies), MIPS (3/8), and ISOCAM images (5/8) of the target galaxies. The beam size is also used to convert the averaged high-resolution spectra to flux intensity units.

### *Effective Integration Times*

All spectra delivered are the composite of multiple exposures. For the high-resolution results, 30 (15) individual DCE's totaling 15.73 min (15.24 min) of integration time were combined to produce a single SH (LH) spectrum. For SL spectra, the full maps required only 8.8 min (4.4 min each for SL1 and SL2), and the majority of the on-order data were averaged together to produce the spectrum. The much larger LL strip maps ranged from 20.97 min to 41.95 min total integration time. The effective integration times per pixel were 58.7 sec in SL, and 125.84 sec in LL. Only 4-7% of the full LL map was used to match the SL extraction region, although 10-20% of the map (taken from the extremities) was also used for background subtraction.

For a given peak source flux, the signal-to-noise in the resulting spectra depends critically on the spatial distribution of the source. For galaxies with significant extended emission in the extraction regions (e.g. NGC5194), the relative S/N achieved is much higher than for galaxies whose mid-infrared flux is concentrated in the nucleus (e.g. NGC5408). In many cases, higher S/N spectra could be achieved by extracting over smaller regions; for consistency all regions were chosen to be the same size.

## **5.4 Known Problems**

### *High-resolution Backgrounds*

The IRS pipeline removes some fraction of the background light implicitly, through the use of a "dark" data product which is created from observations of a dark patch in the zodiacal foreground. The correct estimation of infrared background will affect, for instance, equivalent line widths measured in the high-resolution spectra.

### *Spectral Mismatch and Astrometric Uncertainty*

The 4 segments of the low-resolution spectra (SL2, SL1, LL2, LL1, in order of increasing wavelength) come from separate spectral cubes. The size and position of the extraction region was hand-matched, because residual 1-3" errors in the astrometry of the cube remain. This means that the precision of the extraction areas reported in the spectral headers have similar uncertainty (1" typical). This can contribute to mismatch between SL and LL, and, to a lesser degree, to mismatch between orders in the same spectral module (SL1 and SL2, LL1 and LL2). A similar issue pertains to the high-resolution spectra. In this case, the region of LH extraction is roughly 4 times as large as the region over which SH was extracted. Depending on the angular distribution of the source flux, this can produce a jump between SH and LH.

### *Order Curvature*

While most high-resolution orders line up very well, significant offsets between orders where they overlap in wavelength and/or residual non-physical curvature in the order data are still visible in some cases. This is most noticeable in the bluest orders of SH and the orders which cover observed wavelengths of 14-17  $\mu\text{m}$ . As the calibration of SH data improves, we expect these residual features to be greatly reduced. In short-high, the red ends of orders 13-20 correspond to an area of decreased responsivity on the array.

### *Extended Source Flux Calibration*

Flux calibration of extended sources is not yet supported by the SSC. In the meantime, we have developed our own corrections necessary to generate fluxes in our spectra. Anticipated improvements to the flux calibration method employed in the IRS pipeline, measurements of the slits' beam profiles, and estimates of the PSF at all wavelengths will all improve the quality of extended source flux estimates. Currently, we estimate our fluxes to be accurate within ~30%.

### *Flux Conversion Errors*

An error in the flux conversion tables (FLUXCON) specific to the pipeline version of the processed raw data used in this delivery (version S10.5a) resulted in FLUXCON-derived fluxes which were low by ~20%. The ALCF is designed to *reduce* the flux of extended sources, for which the native extraction aperture is larger than the narrow aperture employed automatically in the IRS pipeline. In this case, however, the ALCF was used simultaneously to correct the 20% flux error, and the difference between extraction apertures used.

### *Residual Time-Varying Pixels*

Responsive but unruly pixels, present in increasing numbers in the LH data, can lead to spurious features in the final extraction. We have made a careful effort to suppress such spurious features, but we strongly encourage checking the 2D BCD data for uncertain line identifications.

### *Wavelength Calibration Errors*

Several issues with the high-resolution wavelength calibration are being tracked by the SSC, and errors as large as .03  $\mu\text{m}$  have been cataloged. We anticipate that these errors will be removed in subsequent pipeline releases.

### *Stray-Light Contamination*

The SL array also contains two small "peak-up" (PU) fields which can lead to stray light contaminating the spectral orders. Present issues with the stray-light correction module employed in the pipeline can cause horizontal bands of over or under correction in the BCD data. As a result, for SL order 1, we standardized on the *FLATAP* data which have not been corrected for straylight. Since SL1 is far from the PU fields, it should not suffer from stray-light contamination. For SL2 order, which sits adjacent to the PU fields, we relied on the stray-light-corrected BCD data. This issue is also slated for resolution with the S11 pipeline.

## 6. Ancillary Data

### 6.1 Optical Imaging

#### *Observations*

Optical images for the galaxies in the SINGS sample were obtained at NOAO, as part of the Legacy Project, over the course of about 3 years (2001-2003). Observations were carried out at both the KPNO 2.1-m and the CTIO 1.5-m telescopes, using standard broad band B, V, R, and I filters, and a set of narrow-band filters in correspondence of the redshifted H $\alpha$  line emission (0.6563  $\mu$ m). For the 8 galaxies in the present delivery, the characteristics of the narrow-band filters (from the NOAO Web pages) are as follows:

Filter Name	Central Wavelength	FWHM	Peak Transmission
KP1563 (KPNO)	6573 A	67 A	83 %
KP1564 (KPNO)	6618 A	74 A	79 %
CT6602 (CTIO)	6596 A	18 A	70 %

The 2Kx2K CCDs used for the observations have field-of-view (FOV) of 10' and 14.5', and pixel scale 0.''305 and 0.''433, at the KPNO-2.1-m and at the CTIO-1.5-m telescopes, respectively. Galaxies more extended than the CCD FOVs were imaged at multiple, overlapping pointings.

Exposure times ranged from 240 seconds to 1400 seconds (typically split into 2 separate exposures for cosmic ray removal.), in order to reach uniform depth of about 25 mag/arcsec<sup>2</sup> with signal-to-noise ratio of  $\sim 10$  in the broad-band filters. Exposure times in the narrow-band filters were typically 1800 seconds, split into two separate exposures.

#### *Data Processing*

Data reduction consisted of bias subtraction (using also the overscan region in the case of the KPNO images), flat-fielding (with both dome- and twilight-flats), single-image cosmic ray removal, and combination of pairs (or multiple) images at the same pointing/filter.

The southern 3' of the CCD FOV at the KPNO-2.1-m suffers from pronounced **vignetting**, whose intensity is pointing-dependent. We developed a routine to remove as much as possible of the vignetting effect from each frame. The corrected frames were then used to create the final mosaics. See the section on 'Known Problems' below for a quantification of the effectiveness of the vignetting-removal routine.

Astrometric solutions were derived for all optical images/mosaics, and the appropriate WCS keywords (FITS standard) stored in the image headers. All

delivered optical images/mosaics have been rotated to the standard NE orientation.

Photometric and spectrophotometric standard stars were observed during each observing run to flux calibrate the images/mosaics. The spectrophotometric stars (e.g., Feige 34, HZ44) were used to obtain flux calibrations for the narrow-band filters. Effects of vignetting were negligible on the standard star frames, as the stars were usually centered on the CCD FOV, thus avoiding the vignetted edge.

### ***Data Characteristics***

All delivered optical images are in units of counts-per-seconds (CPS, stored in the UNITS keyword). The flux conversion keyword is PHOTFLAM, with units of Jy\*sec/DN/pixel, as given by the keyword ZUNITS. Zeropoints are stored in the keyword ZPOINT (in Jy).

The images in this delivery are **not** background-subtracted. The narrow-band images generally contain emission from H $\alpha$ , as well as the [NII]( $\lambda\lambda$  6548,6584), along with underlying stellar continuum. Users can construct pure emission-line images by scaling and subtracting the R-band images.

The accuracy of the calibration (i.e., to account for non-photometric nights, uncertainties in the calibrations of standard stars, etc.) is provided in the image header of each frame, as a COMMENT keyword. When more than one comment line is present, suffixes (COMMENT1, COMMENT2, etc.) are used. For a fully photometric night, and with the best standard calibrators, a photometric accuracy of ~5% and 10% for broad-band and narrow-band filters respectively, is achieved.

In addition to astrometric and photometric keywords, the image headers contain other useful keywords detailing the observations (e.g., telescope, camera, filters, exposure times, etc.).

### ***Conversion from count-rates to fluxes/magnitudes***

Conversions from count-rates (CPS) to standard (Vega) magnitude scales for the optical images are accomplished with the following formula:

$$m = -2.5 * [\log(\text{CPS} * \text{PHOTFLAM}) - \log(\text{ZPOINT})]$$

To convert continuum-subtracted narrow-band images from CPS to more familiar units for emission lines, e.g., erg s<sup>-1</sup> cm<sup>-2</sup>:

$$F(\text{erg s}^{-1} \text{ cm}^{-2}) = 3\text{E-}5 * \text{CPS} * \text{PHOTFLAM} * \text{FWHM} / \text{CW}^2$$

where FWHM and CW are the full-width half maximum and the central wavelength of the narrow-band filter, respectively. If the emission line(s) are shifted from the center of the filter's bandwidth, additional corrections for the filter's transmission curve need to be included in the above formula.



### ***Known Problems***

Comparison of the fluxes of stars in common between adjacent, overlapping pointings indicate that the vignetting-correction routine usually brings stellar fluxes into agreement within 2%-3%, but deviations as large as 5%-10% are not uncommon. Such residuals are often visible as 'seams' at the overlapping points of adjacent frames.

#### *Notes on individual galaxies:*

*NGC2798:* residual fixed pattern noise present in all images. This is present in both unreduced and reduced images, and in the dark and bias frames as well.

*NGC3198:* Marginal seeing conditions (broad PSF).

*NGC4725:* Only the NE frame is available for the B band.

*NGC4826:* Optical images are from the SONG collaboration. The pixel scale is approximately 0.777 arcsec/pixel. The Ha image is already continuum-subtracted (information stored in the image header as COMMENT\* keyword). A few bad columns (190-195) have been interpolated across, for the B, V, R, and I images. No calibration scales could be obtained for the R and I bands. No zeropoints available.

*NGC5194:* In addition to the nominal mosaics, a set of short-exposure mosaics are delivered for the V, R, and I bands, to aid treatment of the saturated nucleus of the galaxy. Residual vignetting is particularly noticeable in the R and I-band images of this galaxy, along the EW seam between the two overlapping pointings, and especially at the western side of the seam. In this latter region, the effect of the residual vignetting translates into an 8% variation in the surface brightness of the galaxy across the seam, at a position located 174 arcsec west of the nucleus. The surface brightness at this location is about 360 times fainter than the nuclear one. The effects of residual vignetting become worse westward of this point, and quickly decrease in magnitude eastward of this point.

## 6.2 Optical Spectroscopy

### *Observations*

Optical spectra for the SINGS galaxies in the wavelength range 0.36-0.70  $\mu\text{m}$ , with resolution  $\sim 8$  Angstrom, were obtained at the 2.3-meter Bok telescope with the B&C spectrograph, and at the 1.5-meter CTIO telescope with CSPEC.

Three types of long-slit spectra were obtained:

- Nuclear spectra: a 2".5 wide aperture (3" at CTIO) was pointed at the brightest central spot of the galaxy;
- 20" drift scans: the slit was drifted for 20" around the central region, while exposing;
- 55" drift scans: similar to the 20" drift scans, with a scan length of 55".

The data were taken during clear, photometric or semi-photometric conditions. A minimum of two sequential exposures were taken to facilitate cosmic-ray rejection. The total exposure times ranged from 600 seconds for the nuclear pointings to 900-2400 seconds for the 20" and 55" drift-scanned spectra. In the drift-scanned spectra the *effective* exposure time,  $t_{\text{effective}}$ , spent on a single spatial position of the galaxy is given by:

$$t_{\text{effective}} = t_{\text{exposure}} * (\text{Aperture} / \text{Delta}),$$

where  $t_{\text{exposure}}$  is the actual exposure time, Delta is the length of the scan in arcseconds (here, 20" or 55"), and Aperture is the slit width in arcseconds (here, 2.5" or 3"; see Kennicutt 1992, ApJS, 79, 255, for details).

### *Data Processing*

The two-dimensional spectra were reduced with iSPEC2d, a customized longslit data reduction package developed in IDL by John Moustakas. The data were overscan- and bias-subtracted, trimmed, flat-fielded, and corrected for a low-order illumination pattern. The two-dimensional sky spectrum was subtracted from each image before rebinning using the technique described in Kelson (2003, PASP, 115, 688). Sequential exposures were combined to reject cosmic rays; residual cosmic rays and hot pixels were flagged using LA\_COSMIC (van Dokkum 2001, PASP, 113, 1420) and interpolated. The data were then wavelength- and flux-calibrated. Although standard stars were taken through good sky and seeing conditions, absolute spectrophotometric accuracy is not guaranteed, especially for the 2.5 arcsec nuclear spectra where slit losses from seeing may be significant. The relative spectrophotometric accuracy ranges from 1-4% based on the relative scatter in the derived sensitivity function. Two-dimensional error maps are generated using the known noise properties of the CCD and assuming Poisson statistics. These error maps are processed identically to the data.

One-dimensional data, error, and sky spectra were extracted in a 2.5" aperture for the nuclear spectra and a 20" aperture for the drift-scanned spectra using a low-order trace. A small wavelength shift was applied to the final wavelength solution by centroiding on

the [O I] 5577 night sky line. The spectra have been de-reddened for foreground Galactic extinction assuming the O'Donnell (1994, ApJ, 422, 158) extinction curve and using the Schlegel, Finkbeiner, & Davis (1998, ApJ, 500, 525) reddening maps. The 20'' drift-scan spectra accompany the equivalent-size extraction 1D IRS spectra.

### ***Data Characteristics***

The data are stored as ASCII files with the following columns:

1 – wavelength	[Angstrom]
2 – sky-subtracted data spectrum	[erg s <sup>-1</sup> cm <sup>-2</sup> Å <sup>-1</sup> ]
3 - error spectrum	[erg s <sup>-1</sup> cm <sup>-2</sup> Å <sup>-1</sup> ]
4 - sky spectrum	[erg s <sup>-1</sup> cm <sup>-2</sup> Å <sup>-1</sup> ]

At the beginning of each file, basic information on the slit center is also reported.

The file names indicate the type of spectrum ("drift" or "nuclear"), the drift scan length, and the extraction aperture in arcseconds. For example, in "ngc\_0337\_drift\_020\_020.txt", the first "020" is the scan-length while the second "020" is the aperture width. In "ngc\_0337\_nuclear\_002.5.txt" only one number appears indicating the extraction aperture.

### ***Notes on individual galaxies:***

*Ngc0337*: Ill-defined nucleus, the tracing (placement of the extraction aperture's center) along the wavelength direction was not optimal.